applied sciences

Article

Adaptive, Observer-Based Synchronization of Different Chaotic Systems

Jacek Kabziński and Przemysław Mosiołek *

Institute of Automatic Control, Lodz University of Technology, Stefanowskiego 18, 90-537 Lodz, Poland; jacek.kabzinski@p.lodz.pl
* Correspondence: przemyslaw.mosiolek@p.lodz.pl

Abstract: In this study, the problem of master–slave synchronization of two different chaotic systems is considered and solved under a novel set of assumptions. The mathematical model of each of them contains unknown, constant parameters. Only a single output of the master system is available, and only a single input of the slave system is a control input. The proposed, novel approach is based on the active cooperation of the adaptive observer of the master system and adaptive controller of the slave. The tuning function technique is included in the observer–controller design to avoid overparameterization. Complexity explosion and unacceptable increases in adaptive parameters are prevented by proper adaptive techniques application. Due to the selected observer type, the derivation is restricted to the defined class of master systems—output-nonlinear parametric (ONP) systems. Linear transformation of several popular chaotic systems (e.g., Arneodo, Arneodo–Coullet, Genesio–Tesi, Lur'e) into the ONP form is discussed. The stability of the whole, closed-loop system is derived using Lyapunov techniques and examples of implementation (synchronization of Arneodo and 3D jerk systems) are provided.

Keywords: adaptive backstepping; chaos synchronization; nonlinear observer

Citation: Kabziński, J.; Mosiołek, P. Adaptive, Observer-Based Synchronization of Different Chaotic Systems. *Appl. Sci.* **2022**, *12*, 3394. https://doi.org/10.3390/app12073394

Academic Editors: Roman Starosta, Jan Awrejcewicz, José A. Tenreiro Machado, José M. Vega, Hari Mohan Srivastava, Ying-Cheng Lai and Hamed Farokhi

Received: 30 January 2022
Accepted: 23 March 2022
Published: 27 March 2022

1. Introduction

As chaotic behavior is so sensitive to initial conditions, it is hard to believe that two chaotic systems may achieve synchronous motion. Fortunately, as it was demonstrated in [1], proper control can solve this problem. Despite 30 years of research, synchronization of chaos remains a hot research theoretical topic and stimulates numerous applications. It is a well-established fact that effective synchronization of chaotic systems is wildly used in secure communication [2–4]. Chaotic motion is observed in chemical processes, and synchronization of chaotic oscillations with periodic motion is crucial for certain chemical technologies [5]. The understanding of chaotic dynamics of biological and ecological systems [6,7] helps to apply proper methods to synchronize chaotic motion and to improve the system welfare, despite the destructive activity of humankind. Chaos synchronization in laser systems [8,9] is investigated because of potential applications in secure communication, new technologies such as chaotic Lidar, or random number generators. The mentioned areas of research on chaos synchronization and control are just a few of many reported.

Especially, synchronization of two quite different chaotic systems is a new, interesting fundamental problem and may lead to important applications [10,11]. Numerous biological systems (such as circulatory and respiratory systems [12]) behave synchronously, although they are quite different, and the achievement of this synchronous behavior determines health or disease. Hence, synchronization of different chaotic systems may be considered as a treatment restoring health and welfare. Synchronization of different chaotic systems will open new opportunities in secure communication and any other applications mentioned above. Any real system's parameters are inevitably perturbed by external factors and cannot be exactly known. Therefore, synchronization of two different chaotic systems in the presence of unknown parameters is more essential and useful in real-life applications, and this problem will be reflected in this contribution.

We can distinguish two main approaches to the synchronization of chaotic systems. The first approach is to propose a proper control for a slave system to follow the desired trajectory, generated by a master system. Numerous control techniques are reported: sliding mode control [13,14], adaptive backstepping [15,16], dynamic surface control (DCS) [17,18], etc. Commonly, measurement of the master system output is not enough to synthesize the controller. Higher derivatives of the master output are usually necessary to synthesize the controller, but these signals are rarely available.

Using the second approach, the slave system is made to be an observer for the master system [19–21]. Therefore, the structure of the slave system is defined by the master system, and the possibilities to synchronize two different chaotic systems are limited.

In this contribution, we connect both approaches by proposing the novel structure shown in Figure 1. The observer provides estimated state variables to contribute to the control law while tracking errors are fed back from the controller to improve the observer.

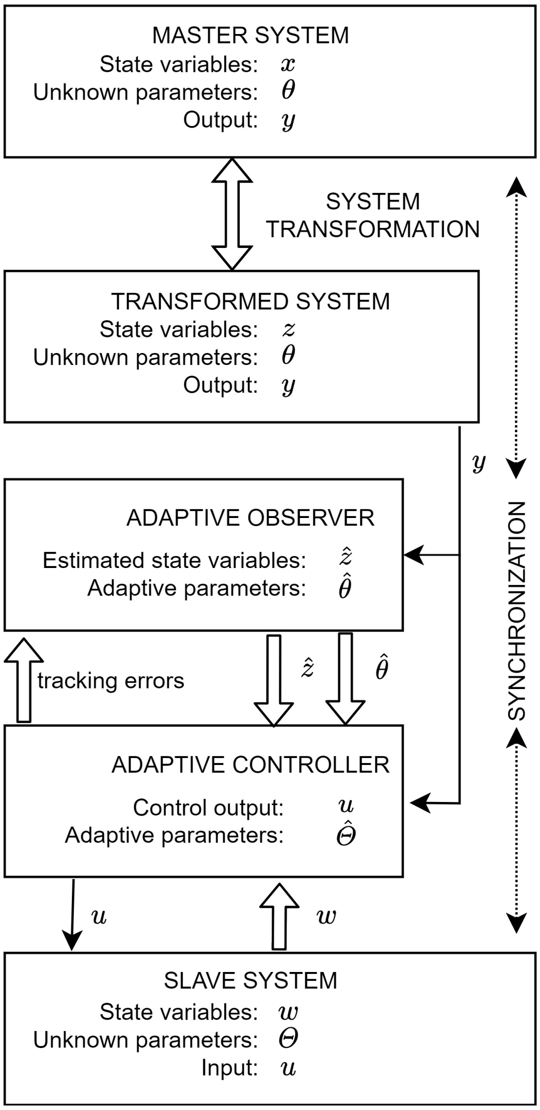

Figure 1. General scheme of the proposed approach.

Several nonlinear adaptive observers are reported in the literature: Luenberger-type observer [22–24], Kalman filter [25], sliding mode observers [26,27], high gain [28,29], etc. Some of them require special conditions for a nonlinear system, for example, Lipschitz-type [30,31] or quadratic-type [32] constraints. After careful consideration, we selected a classical solution reported in [33] based on K filters presented in [34]. Such observers are smooth and free from application difficulties common for sliding mode and high-gain observers, do not require any global constraints for system nonlinearities (as it is assumed in [35], for example), and a linear approximation of system nonlinearities (as in [36]) is not necessary. On the other hand, the system must be transformed into a special canonical form depicted in Figure 1.

Finally, the problem of chaotic systems synchronization is solved under the following assumptions:

- Master and slave systems may be different;
- Master and slave systems contain (different) unknown, constant parameters;
- Only the single output of the master system is available;
- The slave system is controlled by a single input located in the last state equation.

According to our knowledge, the problem of chaos synchronization under such a set of assumptions has never been investigated previously. Additionally, the design methodology applied here is a new approach. First, we construct an adaptive observer based on a nonlinear state transformation and K filters. In contrast to the original observer shown in [33], we introduce a component related to the control algorithm into the observer's equations. This new approach enables observer–controller cooperation, improving synchronization performance as the final effect. The tuning function technique [37] is smartly included in the observer–controller design to avoid overparameterization.

The paper is organized as follows: Output nonlinear parametric (ONP) systems are defined in Section 2, and the observer for such systems is described and modified to enable cooperation with the tracking controller. Next, we discuss chaotic systems transformable into the ONP form by a linear transformation. Several popular systems such as Arneodo [11], Arneodo–Coullet [38], Genesio–Tesi [39], and Lur'e [35] belong to this class. The general form of transformation is provided in the Appendix A. In Section 4, we define a slave system and the synchronization problem. We concentrate on third-order systems, although generalization of the proposed design technique is possible. Section 5 is devoted to the closed-loop adaptive controller design. The stability of the whole system is discussed in Section 6. Finally, examples, discussion, and conclusions are presented.

2. Adaptive Observer for an Output Nonlinear Parametric System

We consider a general nonlinear system (nonlinear in states and inputs), but we assume that it is transformable (by a certain nonlinear state transformation, which may depend on unknown parameters) into a nonlinear system described by state and output equations as follows:

$$\dot{\boldsymbol{z}} = \boldsymbol{A}\boldsymbol{z} + \boldsymbol{\varphi}(y, \boldsymbol{r}) + \boldsymbol{F}(y, \boldsymbol{r})^T \boldsymbol{\theta} \tag{1}$$

$$y = \boldsymbol{c}^T \boldsymbol{z}, \tag{2}$$

where $\boldsymbol{z}$ denotes a vector of n state variables; y is a scalar, measurable output; $\boldsymbol{r}$ is an external, measurable input. The matrices $\boldsymbol{A}, \boldsymbol{c}^{\boldsymbol{T}}$ of appropriate dimensions $(n \times n, 1 \times n)$ are known, as well as nonlinear functions $\boldsymbol{\varphi}(y, \boldsymbol{r}), \boldsymbol{F}(y, \boldsymbol{r})$, while $\boldsymbol{\theta}$ represents a vector of p unknown, constant, bounded parameters. The design of an adaptive observer for the system (1), (2) is discussed in this section.

Let us call the assumed system model (1), (2) an output-nonlinear parametric system (ONP). The model (1), (2) is restrictive as the nonlinearities and terms with unknown parameters in the state equation depend on the measured signals only (that is why we call it output-nonlinear). We have to stress that this restriction is not imposed because of the adaptive control. Even if the parameters are known, the class of systems globally stabilizable by output feedback is not much wider than the class provided by (1), (2) [33,40]. Despite this, many important chaotic systems may be transformed to the form (1), (2), so we claim that the proposed approach is general enough. The system form (1), (2) corresponds with the selected observer design technique, and this was widely discussed and compared with other opportunities in Section 1. The features of ONP systems and the systems transformable into the ONP form are an interesting research topic, although outside the scope of this paper. Let us mention that the system obtained by a linear state transformation from any ONP system remains in the ONP form.

The system (1), (2) may be chaotic or not. We assume that there exists an output–feedback–gain matrix $\boldsymbol{k}$, such that $\boldsymbol{A_o} := \boldsymbol{A} - \boldsymbol{k}\boldsymbol{c}^T$ is stable, and therefore, for any positive definite matrix $\boldsymbol{Q}$, the Lyapunov equation

$$\boldsymbol{A}_{\boldsymbol{o}}^T\boldsymbol{R} + \boldsymbol{R}\boldsymbol{A_o} = -\boldsymbol{Q} \tag{3}$$

possesses a positive definite solution $\boldsymbol{R}$. Of course, working with a single output system ($\boldsymbol{k}$ is a column vector with n parameters) is a special case of multidimensional output. Multioutput case means that more than n feedback parameters may be used to satisfy (3). Therefore, the single output is the most restrictive case. Transmission of a single signal is also an advantage in secure communication, which is the main application field of chaos synchronization.

Motivated by the idea of K filters presented in [33,34], we introduce an observer, so that we are able to reconstruct the state variables $\boldsymbol{z}$ despite unknown parameters $\boldsymbol{\theta}$.

Let us define the observer state variables $\hat{\boldsymbol{z}}$ and the observer state equation as

$$\dot{\hat{\boldsymbol{z}}} = \boldsymbol{A_o}\hat{\boldsymbol{z}} + \boldsymbol{\varphi}(y, \boldsymbol{r}) + \boldsymbol{k}y + \boldsymbol{P}^T\dot{\hat{\boldsymbol{\theta}}} + \boldsymbol{F}(y, \boldsymbol{r})^T\hat{\boldsymbol{\theta}} + \boldsymbol{s} \tag{4}$$

where

- The $p \times n$ matrix variable $\boldsymbol{P}$ is an output of a linear filter to be defined;
- The unknown parameters $\boldsymbol{\theta}$ are substituted by adaptive parameters $\hat{\boldsymbol{\theta}}$, tuned according to adaptive law

$$\dot{\hat{\boldsymbol{\theta}}} = \boldsymbol{\Gamma}\boldsymbol{P}\boldsymbol{c}e_1 - \boldsymbol{\Gamma}\boldsymbol{\tau_1} \tag{5}$$

where $e_1 := y - \boldsymbol{c}^{\boldsymbol{T}}\hat{\boldsymbol{z}}$; $\boldsymbol{\Gamma}$ is a symmetric, positive definite matrix of design parameters;

- The component $\boldsymbol{s}$ and the tuning function $\boldsymbol{\tau_1}$ are used to modify the observer dynamics according to the slave system tracking errors, and meanwhile may be assumed equal to zero.

The adaptive law (5) will be justified by the analysis of the Lyapunov function including the complete closed-loop system. The form of (5) is standard: It contains a component with an observer error e_1 and a tuning component $\boldsymbol{\tau_1}$, which is used to avoid overparameterization. In this way, the observer is prepared for cooperation with the adaptive tracking controller of a slave system, although at this moment, the specific choice of (5) is not necessary.

We denote the state estimation error as

$$\boldsymbol{e} = \boldsymbol{z} - \hat{\boldsymbol{z}}, \tag{6}$$

the parameter adaptation error as

$$\tilde{\boldsymbol{\theta}} = \boldsymbol{\theta} - \hat{\boldsymbol{\theta}}, \tag{7}$$

and the "composite" error as

$$\boldsymbol{\varepsilon} = \boldsymbol{e} - \boldsymbol{P}^{\boldsymbol{T}}\tilde{\boldsymbol{\theta}}. \tag{8}$$

Differentiation of (8) performed after plugging in (1), (4), and $\dot{\tilde{\boldsymbol{\theta}}} = -\dot{\hat{\boldsymbol{\theta}}}$ provides that the time derivative of $\boldsymbol{\varepsilon}$ is given by

$$\begin{aligned} \dot{\boldsymbol{\varepsilon}} = \dot{\boldsymbol{z}} - \dot{\hat{\boldsymbol{z}}} - \dot{\boldsymbol{P}}^T\widetilde{\boldsymbol{\theta}} + \boldsymbol{P}^T\dot{\hat{\boldsymbol{\theta}}} = \boldsymbol{A}\boldsymbol{z} + \boldsymbol{\varphi}(y,\boldsymbol{r}) + \boldsymbol{F}(y,\boldsymbol{r})^T\boldsymbol{\theta} \\ -\left[\boldsymbol{A_o}\hat{\boldsymbol{z}} + \boldsymbol{\varphi}(y,\boldsymbol{r}) + \boldsymbol{k}\boldsymbol{c}^T\boldsymbol{z} + \boldsymbol{P}^T\dot{\hat{\boldsymbol{\theta}}} + \boldsymbol{F}(y,\boldsymbol{r})^T\hat{\boldsymbol{\theta}} + \boldsymbol{s}\right] \\ -\dot{\boldsymbol{P}}^T\widetilde{\boldsymbol{\theta}} + \boldsymbol{P}^T\dot{\hat{\boldsymbol{\theta}}} = \boldsymbol{A_o}\boldsymbol{e} + \boldsymbol{F}(y,\boldsymbol{r})^T\widetilde{\boldsymbol{\theta}} - \boldsymbol{s} - \dot{\boldsymbol{P}}^T\widetilde{\boldsymbol{\theta}}. \end{aligned} \tag{9}$$

Therefore, if the $p \times n$ matrix variable $\boldsymbol{P}$ is modified according to the differential equation,

$$\dot{\boldsymbol{P}}^T = \boldsymbol{A_o}\boldsymbol{P}^T + \boldsymbol{F}(y,\boldsymbol{r})^T, \tag{10}$$

we obtain from (9)

$$\dot{\boldsymbol{\varepsilon}} = \boldsymbol{A_o}\boldsymbol{\varepsilon} - \boldsymbol{s}, \tag{11}$$

and this result does not depend on any specific adaptive law (5). Hence, in the non-adaptive case, when $\widetilde{\boldsymbol{\theta}} = \boldsymbol{0}, \boldsymbol{s} = 0$, the error $\boldsymbol{\varepsilon} = \boldsymbol{e}$ converges to zero for any initial value of $\boldsymbol{e}$.

For the adaptive case, we may use the Lyapunov function

$$V = \boldsymbol{\varepsilon}^{\boldsymbol{T}}\boldsymbol{R}\boldsymbol{\varepsilon} + \frac{1}{2}\widetilde{\boldsymbol{\theta}}^{\boldsymbol{T}}\boldsymbol{\Gamma}^{-\boldsymbol{1}}\widetilde{\boldsymbol{\theta}}, \tag{12}$$

which is positive definite as a function of $\boldsymbol{e}, \widetilde{\boldsymbol{\theta}}$. For $\boldsymbol{\tau_1} = \boldsymbol{0}$ and $\boldsymbol{s} = \boldsymbol{0}$, as $\widetilde{\boldsymbol{\theta}}^{\boldsymbol{T}}\boldsymbol{P}\boldsymbol{c} = \boldsymbol{c}^{\boldsymbol{T}}\boldsymbol{P}^{\boldsymbol{T}}\widetilde{\boldsymbol{\theta}} = e_1 - \boldsymbol{c}^{\boldsymbol{T}}\boldsymbol{\varepsilon}$, we obtain

$$\begin{aligned} \dot{V} &= \dot{\boldsymbol{\varepsilon}}^T\boldsymbol{R}\boldsymbol{\varepsilon} + \boldsymbol{\varepsilon}^T\boldsymbol{R}\dot{\boldsymbol{\varepsilon}} + \widetilde{\boldsymbol{\theta}}^T\boldsymbol{\Gamma}^{-\boldsymbol{1}}\dot{\widetilde{\boldsymbol{\theta}}} = \boldsymbol{\varepsilon}^T\boldsymbol{A_o}^T\boldsymbol{R}\boldsymbol{\varepsilon} + \boldsymbol{\varepsilon}^T\boldsymbol{R}\boldsymbol{A_o}\boldsymbol{\varepsilon} - \widetilde{\boldsymbol{\theta}}^T\boldsymbol{\Gamma}^{-\boldsymbol{1}}\dot{\hat{\boldsymbol{\theta}}} = -\boldsymbol{\varepsilon}^T\boldsymbol{Q}\boldsymbol{\varepsilon} - \widetilde{\boldsymbol{\theta}}^T\boldsymbol{P}\boldsymbol{c}e_1 \\ &= -\boldsymbol{\varepsilon}^T\boldsymbol{Q}\boldsymbol{\varepsilon} - e_1^2 + \boldsymbol{c}^T\boldsymbol{\varepsilon}e_1 = -\boldsymbol{\varepsilon}^T\boldsymbol{Q}\boldsymbol{\varepsilon} + \frac{1}{2}(\boldsymbol{c}^T\boldsymbol{\varepsilon})^2 - \frac{1}{2}e_1^2 - \frac{1}{2}e_1^2 - \frac{1}{2}(\boldsymbol{c}^T\boldsymbol{\varepsilon})^2 + \boldsymbol{c}^T\boldsymbol{\varepsilon}e_1 \\ &= -\boldsymbol{\varepsilon}^T\left(\boldsymbol{Q} - \frac{1}{2}\boldsymbol{c}\boldsymbol{c}^T\right)\boldsymbol{\varepsilon} - \frac{1}{2}e_1^2 - \frac{1}{2}(e_1 - \boldsymbol{c}^T\boldsymbol{\varepsilon})^2. \end{aligned} \tag{13}$$

The standard reasoning, commonly used in adaptive control and presented in [41,42] is applied to make conclusions from (13): The Lyapunov function derivative is negative except the set $M = \{(\boldsymbol{e}, \widetilde{\boldsymbol{\theta}}): \boldsymbol{e} - \boldsymbol{P}^T\widetilde{\boldsymbol{\theta}} = \boldsymbol{0}, e_1 = 0\}$. Therefore, we determine that $\boldsymbol{\varepsilon} \to \boldsymbol{0}$ and $\widetilde{\boldsymbol{\theta}}$ is bounded, and analyzing the set M, assuming the persistency of excitation of $\boldsymbol{P}\boldsymbol{c}\boldsymbol{c}^T\boldsymbol{P}^T$, we find that $\boldsymbol{e} = \boldsymbol{0}, \widetilde{\boldsymbol{\theta}} = \boldsymbol{0}$ is the only possible trajectory in M; hence, $\boldsymbol{e} \to \boldsymbol{0}, \widetilde{\boldsymbol{\theta}} \to \boldsymbol{0}$. As a matter of fact, in the adaptive case, we consider the tracking, closed-loop system stability rather than the observer alone.

3. Master Chaotic Systems Transformable into ONP Form

General, necessary, and sufficient conditions for the existence of local change in coordinates $\boldsymbol{z} = \boldsymbol{\Phi}(\boldsymbol{x})$ transforming a nonlinear system

$$\dot{\boldsymbol{x}} = \boldsymbol{f}(\boldsymbol{x}) + \boldsymbol{f_0}(\boldsymbol{x},\boldsymbol{u}) + \boldsymbol{\theta}^T\boldsymbol{f}(\boldsymbol{x},\boldsymbol{u}) \tag{14}$$

with parameters $\boldsymbol{\theta}$ into the ONP form (1), (2) are given in [33,43]. In this contribution, we concentrated on third-order chaotic systems transformable into the ONP form. For example, consider shifted Arneodo system

$$\begin{aligned} \dot{x}_1 &= x_2, \\ \dot{x}_2 &= x_3, \\ \dot{x}_3 &= a(x_1 + r) - bx_2 - x_3 - (x_1 + r)^2, \end{aligned} \tag{15}$$

which is a classical Arneodo system for $r = 0$, chaotic for a certain subset of parameters (a, b) [11]. The system (15) is transformed by a linear transformation

$$\boldsymbol{z} = \boldsymbol{\Phi}(a,b)\boldsymbol{x}, \qquad \boldsymbol{\Phi}(a,b) = \begin{bmatrix} 1 & 0 & 0 \\ 1 & 1 & 0 \\ b & 1 & 1 \end{bmatrix} \tag{16}$$

into the ONP form

$$\begin{aligned}\dot{z}_1 &= -z_1 + z_2,\\ \dot{z}_2 &= -bz_1 + z_3,\\ \dot{z}_3 &= a(z_1 + r) - (z_1 + r)^2\end{aligned} \tag{17}$$

(see Appendix A for more details). Assuming that the output is $y = z_1 = x_1$, and comparing with (1), (2), we obtain:

$$\boldsymbol{A} = \begin{bmatrix} 0 & 1 & 0 \\ 0 & 0 & 1 \\ 0 & 0 & 0 \end{bmatrix}; \quad \boldsymbol{\varphi}(y, r) = \begin{bmatrix} -y \\ 0 \\ -(y + r)^2 \end{bmatrix}; \ \boldsymbol{F}(y, \boldsymbol{r})^T = \begin{bmatrix} 0 & 0 \\ 0 & -y \\ y + r & 0 \end{bmatrix};$$
$$\boldsymbol{\theta} = \begin{bmatrix} a \\ b \end{bmatrix}; \ \boldsymbol{c}^T = [1\ 0\ 0]. \tag{18}$$

The inverse transformation is given by:\

$$\boldsymbol{x} = \boldsymbol{\Phi}^{-1}(\boldsymbol{\theta})\boldsymbol{z}, \qquad \boldsymbol{\Phi}^{-1}(\boldsymbol{\theta}) = \begin{bmatrix} 1 & 0 & 0 \\ -1 & 1 & 0 \\ 1 - b & -1 & 1 \end{bmatrix}. \tag{19}$$

Motivated by this example, we consider as a master system any third-order nonlinear system with state variables $\boldsymbol{x}$, the output $y = x_1$, and unknown constant parameters $\boldsymbol{\theta}$, given by

$$\begin{aligned}\dot{x}_1 &= x_2,\\ \dot{x}_2 &= x_3,\\ \dot{x}_3 &= f_0(\boldsymbol{x}, r) + \boldsymbol{\theta}^T \boldsymbol{f}(\boldsymbol{x}, r),\end{aligned} \tag{20}$$

and transformable into the ONP form (1), (2), assuming that the inverse transformation is given by:

$$\begin{aligned}x_1 &= z_1,\\ x_2 &= \boldsymbol{\alpha}^T \boldsymbol{z},\\ x_3 &= \boldsymbol{\beta}_0^T \boldsymbol{z} + \sum_{i=1}^{p} \theta_i \boldsymbol{\beta}_i^T \boldsymbol{z},\end{aligned} \tag{21}$$

where vectors $\boldsymbol{\alpha}^T, \boldsymbol{\beta}_i^T$ are constant and θ_i are unknown, constant parameters.

As the output $y = z_1 = x_1$ is available, we construct an observer (4) for the ONP system (1), (2).

4. Slave System

The slave system is assumed to be a third-order chaotic system given by

$$\begin{aligned}\dot{w}_1 &= w_2,\\ \dot{w}_2 &= w_3,\\ \dot{w}_3 &= \boldsymbol{\Theta}^T \boldsymbol{H}(\boldsymbol{w}) + h(\boldsymbol{w}) + u,\end{aligned} \tag{22}$$

with $\bar{p}$ unknown, constant, bounded parameters $\boldsymbol{\Theta}$, known nonlinearities $\boldsymbol{H}(\boldsymbol{w}), h(\boldsymbol{w})$ of proper dimensions $(\bar{p} \times 1, 1 \times 1)$, measurable state variables and the control input u. An exemplary slave system may be a 3D jerk chaotic system [44]. In this case, we have

$$= \begin{bmatrix} a \\ b \\ c \end{bmatrix}, \quad \boldsymbol{H}(\boldsymbol{w}) = \begin{bmatrix} -w_3 \\ -w_1 \\ w_2 \end{bmatrix}, \qquad h(\boldsymbol{w}) = w_1 w_2^2 - w_1^3. \tag{23}$$

The aim of the control is to make the slave signal w_1 follow the bounded output y generated by the master system, in spite of unknown parameters $\boldsymbol{\theta}$ (in the master system) and $\boldsymbol{\Theta}$ (in the slave system).

5. Adaptive Control

The adaptive backstepping with the tuning function approach was used to derive the synchronizing controller. To make the derivation more readable, we collected all important signals and parameters, which are listed in Table 1.

Table 1. Important signals and parameters.

Adaptive Observer		Adaptive Controller	
$\hat{\boldsymbol{z}}$	Estimated state variables	v_1	Synchronization error, first-loop tracking error
$\boldsymbol{e}$	Estimation error	w_{2d}	First-loop stabilizing function (desired trajectory for w_2)
e_1	First-state variable estimation error	v_2	Tracking error for w_2
$\boldsymbol{\varepsilon}$	"Composite" error	w_{3d}	Second-loop stabilizing function (desired trajectory for w_3)
$\hat{\boldsymbol{\theta}}, \tilde{\boldsymbol{\theta}}$	Adaptive parameters and adaptation error	v_3	Tracking error for w_3
$\boldsymbol{P}$	Auxiliary matrix variable	ω	Filter state variable
$\boldsymbol{k}$	Design matrix responsible for observer dynamics	v_{3f}	Filter tracking error
$\boldsymbol{Q}, \boldsymbol{R}$	Auxiliary positive definite matrices used to construct Lyapunov functions	$x_i - w_i$, $i = 1,2,3$	Synchronization errors
$\boldsymbol{\Gamma}, \sigma$	Design parameters responsible for adaptation	u	Control input
$\boldsymbol{\tau_1}, \boldsymbol{s}, \boldsymbol{\tau_2}, \boldsymbol{s_1}$	Corrective signals from adaptive controller	$\hat{\boldsymbol{\Theta}}, \tilde{\boldsymbol{\Theta}}$	Adaptive parameters and adaptation error
		K_1, K_2, K_3	Design parameters shaping trajectories of v_1, v_2, v_{3f}
		Ω	Filter parameter
		$\boldsymbol{\Gamma}_1, \sigma_1$	Design parameters responsible for adaptation

5.1. STAGE 1

Let us denote the tracking error (also synchronization error) by

$$v_1 = x_1 - w_1 \tag{24}$$

and observe that

$$\dot{v}_1 = \dot{x}_1 - \dot{w}_1 = x_2 - w_2 \tag{25}$$

may be represented as

$$\dot{v}_1 = \boldsymbol{\alpha}^T \boldsymbol{z} - w_2 = \boldsymbol{\alpha}^T \left(\hat{\boldsymbol{z}} + \boldsymbol{\varepsilon} + \boldsymbol{P}^{\boldsymbol{T}} \tilde{\boldsymbol{\theta}} \right) - w_2 \tag{26}$$

(because it follows from (6) and (8) that $\boldsymbol{z} = \hat{\boldsymbol{z}} + \boldsymbol{\varepsilon} + \boldsymbol{P}^{\boldsymbol{T}} \tilde{\boldsymbol{\theta}}$).

Let w_{2d} denote the desired trajectory of w_2, which acts as a virtual control in (26). The tracking error for w_2 is defined by

$$v_2 = w_{2d} - w_2. \tag{27}$$

After selecting

$$w_{2d} = \boldsymbol{\alpha}^{\boldsymbol{T}} \hat{\boldsymbol{z}} + K_1 v_1, \tag{28}$$

with a positive design parameter K_1, the error dynamics Equation (26) becomes

$$\dot{v}_1 = -K_1 v_1 + \boldsymbol{\alpha}^T \left(\boldsymbol{\varepsilon} + \boldsymbol{P}^T \tilde{\boldsymbol{\theta}} \right) + v_2 \tag{29}$$

The tuning function $\boldsymbol{\tau_1}$ in (5) and the component $\boldsymbol{s}$ in (4) are selected from the analysis of Lyapunov function

$$V_1 = V + \frac{1}{2}v_1^2 = \boldsymbol{\varepsilon}^T\boldsymbol{R}\boldsymbol{\varepsilon} + \frac{1}{2}\widetilde{\boldsymbol{\theta}}^T\boldsymbol{\Gamma}^{-1}\widetilde{\boldsymbol{\theta}} + \frac{1}{2}v_1^2 \tag{30}$$

Taking $\boldsymbol{\tau_1}$ and $\boldsymbol{s}$ into account leads us to have, instead of (13), the following equation:

$$\dot{V} = -\boldsymbol{\varepsilon}^T\left(\boldsymbol{Q} - \frac{1}{2}\boldsymbol{c}\boldsymbol{c}^T\right)\boldsymbol{\varepsilon} - \frac{1}{2}e_1^2 - \frac{1}{2}(e_1 - \boldsymbol{c}^T\boldsymbol{\varepsilon})^2 + \widetilde{\boldsymbol{\theta}}^T\boldsymbol{\tau}_1 - 2\boldsymbol{\varepsilon}^T\boldsymbol{R}\boldsymbol{s} \tag{31}$$

Therefore, as $\dot{V}_1 = \dot{V} + v_1\dot{v}_1$,

$$\begin{aligned}\dot{V}_1 = -\boldsymbol{\varepsilon}^T\left(\boldsymbol{Q} - \frac{1}{2}\boldsymbol{c}\boldsymbol{c}^T\right)\boldsymbol{\varepsilon} - \frac{1}{2}e_1^2 - \frac{1}{2}(e_1 - \boldsymbol{c}^T\boldsymbol{\varepsilon})^2 + \widetilde{\boldsymbol{\theta}}^T\boldsymbol{\tau}_1 - 2\boldsymbol{\varepsilon}^T\boldsymbol{R}\boldsymbol{s} \\ - v_1\left(K_1v_1 - \boldsymbol{\alpha}^T\left(\boldsymbol{\varepsilon} + \boldsymbol{P}^T\widetilde{\boldsymbol{\theta}}\right) - v_2\right),\end{aligned} \tag{32}$$

and this will be simplified by selecting

$$\boldsymbol{\tau_1} = -\boldsymbol{P}\boldsymbol{\alpha}v_1 + \boldsymbol{\tau_2}, \tag{33}$$

where $\boldsymbol{\tau}_2$ is the next-loop tuning function, and

$$\boldsymbol{s} = \frac{1}{2}\boldsymbol{R}^{-1}(\boldsymbol{\alpha}v_1 + \boldsymbol{s_1}) \tag{34}$$

($\boldsymbol{\tau}_2$ and $\boldsymbol{s}_1$ will be defined in the next stage). Finally,

$$\dot{V}_1 = -\boldsymbol{\varepsilon}^T\left(\boldsymbol{Q} - \frac{1}{2}\boldsymbol{c}\boldsymbol{c}^T\right)\boldsymbol{\varepsilon} - \frac{1}{2}e_1^2 - \frac{1}{2}(e_1 - \boldsymbol{c}^T\boldsymbol{\varepsilon})^2 - K_1v_1^2 + \widetilde{\boldsymbol{\theta}}^T\boldsymbol{\tau_2} + v_1v_2 - \boldsymbol{\varepsilon}^T\boldsymbol{s_1}. \tag{35}$$

5.2. STAGE 2

As $\dot{v}_2 = \dot{w}_{2d} - \dot{w}_2$, using (28), (4), (29), (34), and (22), together with representing virtual control w_3 as

$$w_3 = w_{3d} - v_3, \tag{36}$$

where w_{3d} is the desired trajectory for w_3 and v_3 denotes the tracking error, provides

$$\begin{aligned}\dot{v}_2 = \boldsymbol{\alpha}^T\dot{\hat{\boldsymbol{z}}} + K_1\dot{v}_1 - \dot{w}_2 = \boldsymbol{\alpha}^T\boldsymbol{A_0}\hat{\boldsymbol{z}} + \boldsymbol{\alpha}^T\left\{\boldsymbol{\varphi}(y,r) + \boldsymbol{k}y + \boldsymbol{F}(y,r)^T\widehat{\boldsymbol{\theta}}\right\} \\ +\boldsymbol{\alpha}^T\boldsymbol{P}^T\underbrace{\left\{\boldsymbol{\Gamma}\boldsymbol{P}\boldsymbol{c}e_1 - \boldsymbol{\Gamma}\underbrace{\{-\boldsymbol{P}\boldsymbol{\alpha}v_1 + \boldsymbol{\tau_2}\}}_{\boldsymbol{\tau_1}}\right\}}_{\dot{\hat{\boldsymbol{\theta}}}} + \boldsymbol{\alpha}^T\left\{\underbrace{\frac{1}{2}\boldsymbol{R}^{-1}(\boldsymbol{\alpha}v_1 + \boldsymbol{s_1})}_{\boldsymbol{s}}\right\} - w_{3d} + v_3 \\ +K_1\underbrace{\left\{-K_1v_1 + \boldsymbol{\alpha}^T\left(\boldsymbol{\varepsilon} + \boldsymbol{P^T}\widetilde{\boldsymbol{\theta}}\right) + v_2\right\}}_{\dot{v}_1} = G + \frac{1}{2}\boldsymbol{\alpha}^T\boldsymbol{R}^{-1}\boldsymbol{s_1} + K_1\boldsymbol{\alpha}^T\left(\boldsymbol{\varepsilon} + \boldsymbol{P}^T\widetilde{\boldsymbol{\theta}}\right) - w_{3d} + v_3,\end{aligned} \tag{37}$$

where

$$G = \boldsymbol{\alpha}^T\left\{\boldsymbol{A_0}\hat{\boldsymbol{z}} + \boldsymbol{\varphi}(y,r) + \boldsymbol{k}y + \boldsymbol{P}^T\left\{\boldsymbol{\Gamma}\boldsymbol{P}\boldsymbol{c}e_1 - \boldsymbol{\Gamma}\{-\boldsymbol{P}\boldsymbol{\alpha}v_1 + \boldsymbol{\tau_2}\}\right\} + \boldsymbol{F}(y,r)^T\widehat{\boldsymbol{\theta}} + \frac{1}{2}\boldsymbol{R}^{-1}\boldsymbol{\alpha}v_1\right\} + K_1v_2. \tag{38}$$

This motivates us to form the desired stabilizing function w_{3d} as

$$w_{3d} = K_2v_2 + G + v_1 + \frac{1}{2}K_1\boldsymbol{\alpha}^T\boldsymbol{R}^{-1}\boldsymbol{\alpha}v_2, \tag{39}$$

with the positive design parameter K_2. The first component in (39) stabilizes the dynamics of v_2, the second compensates for the nonlinearities, and the two last equations are used to cancel some unnecessary terms in the Lyapunov function derivative. Finally, (37) is simplified to

$$\dot{v}_2 = -K_2v_2 - v_1 + \frac{1}{2}\boldsymbol{\alpha}^T\boldsymbol{R}^{-1}\boldsymbol{s_1} - \frac{1}{2}\boldsymbol{\alpha}^T\boldsymbol{R}^{-1}\boldsymbol{\alpha}v_2 + K_1\boldsymbol{\alpha}^T\left(\boldsymbol{\varepsilon} + \boldsymbol{P}^T\widetilde{\boldsymbol{\theta}}\right) + v_3. \tag{40}$$

The Lyapunov function mentioned above is selected as

$$V_2 = V_1 + \frac{1}{2}v_2^2 = \frac{1}{2}v_1^2 + \frac{1}{2}v_2^2 + \frac{1}{2}\tilde{\boldsymbol{\theta}}^T\boldsymbol{\Gamma}^{-1}\tilde{\boldsymbol{\theta}} + \boldsymbol{\varepsilon}^T\boldsymbol{R}\boldsymbol{\varepsilon}, \quad (41)$$

where V_1 is as defined in (30). Plugging in $\dot{V}_1$ from (35) and $\dot{v}_2$ from (40) into $\dot{V}_2 = \dot{V}_1 + v_2\dot{v}_2$ results in

$$\begin{aligned}\dot{V}_2 = &-\boldsymbol{\varepsilon}^T\left(\boldsymbol{Q} - \frac{1}{2}\boldsymbol{c}\boldsymbol{c}^T\right)\boldsymbol{\varepsilon} - \frac{1}{2}e_1^2 - \frac{1}{2}(e_1 - \boldsymbol{c}^T\boldsymbol{\varepsilon})^2 - K_1v_1^2 + \tilde{\boldsymbol{\theta}}^T\boldsymbol{\tau_2} + v_1v_2 - \boldsymbol{\varepsilon}^T\boldsymbol{s_1} - K_2v_2^2 \\ &-v_1v_2 + \frac{1}{2}v_2\boldsymbol{\alpha}^T\boldsymbol{R}^{-1}\boldsymbol{s_1} - \frac{1}{2}K_1\boldsymbol{\alpha}^T\boldsymbol{R}^{-1}\boldsymbol{\alpha}v_2^2 + K_1v_2\boldsymbol{\alpha}^T\left(\boldsymbol{\varepsilon} + \boldsymbol{P}^T\tilde{\boldsymbol{\theta}}\right) + v_2v_3.\end{aligned} \quad (42)$$

Selecting

$$\boldsymbol{s_1} = K_1\boldsymbol{\alpha}v_2 \quad (43)$$

cancels $K_1v_2\boldsymbol{\alpha}^T\boldsymbol{\varepsilon}$ by $\boldsymbol{\varepsilon}^T\boldsymbol{s_1}$**,** and $0.5v_2\boldsymbol{\alpha}^T\boldsymbol{R}^{-1}\boldsymbol{s_1}$ is canceled by the term $0.5K_1\boldsymbol{\alpha}^T\boldsymbol{R}^{-1}\boldsymbol{\alpha}v_2^2$, which was intentionally initiated in (39).

The tunning function $\boldsymbol{\tau_2}$ is used to cancel components containing $\tilde{\boldsymbol{\theta}}$ in (42); therefore,

$$\boldsymbol{\tau_2} = -K_1v_2\boldsymbol{P}\boldsymbol{\alpha} + \sigma\hat{\boldsymbol{\theta}}, \quad (44)$$

where $\sigma > 0$ is a small design parameter. Such a choice of $\boldsymbol{\tau}_2$ changes the adaptive law (5) into $\dot{\hat{\boldsymbol{\theta}}} = \boldsymbol{\Gamma}\boldsymbol{P}(\boldsymbol{c}e_1 + \boldsymbol{\alpha}v_1 + K_1\boldsymbol{\alpha}v_2) - \sigma\boldsymbol{\Gamma}\hat{\boldsymbol{\theta}}$ including a term $-\sigma\boldsymbol{\Gamma}\hat{\boldsymbol{\theta}}$**,** which makes the adaptation more robust. Due to this simplification, UUB stability will be proven instead of asymptotic stability. Finally,

$$\dot{V}_2 = -\boldsymbol{\varepsilon}^T\left(\boldsymbol{Q} - \frac{1}{2}\boldsymbol{c}\boldsymbol{c}^T\right)\boldsymbol{\varepsilon} - \frac{1}{2}e_1^2 - K_1v_1^2 - \frac{1}{2}(e_1 - \boldsymbol{c}^T\boldsymbol{\varepsilon})^2 - K_2v_2^2 + +v_3v_2 + \sigma\tilde{\boldsymbol{\theta}}^T\hat{\boldsymbol{\theta}}. \quad (45)$$

5.3. STAGE 3

Considering (39), the time derivative $\dot{w}_{3d}$ is rather complicated, although it is not impossible to write it down in an explicit form. Obtaining approximation of this derivative from a linear filter

$$\dot{\omega} = \Omega(w_{3d} - \omega) \quad (46)$$

(where ω is the filter state variable, and Ω denotes the filter parameter) allows simplification of the controller. The filter output ω is the response of a stable linear system (46) to the input w_{3d}; therefore, $w_{3d} - \omega$ is bounded, for example, $(w_{3d} - \omega)^2 \leq \rho$.

The filter tracking error is denoted by

$$v_{3f} = \omega - w_3 \quad (47)$$

and this, together with (36), allows us to use $v_3 = w_{3d} + v_{3f} - \omega$ and to express (45) as

$$\begin{aligned}\dot{V}_2 = &-\boldsymbol{\varepsilon}^T\left(\boldsymbol{Q} - \frac{1}{2}\boldsymbol{c}\boldsymbol{c}^T\right)\boldsymbol{\varepsilon} - \frac{1}{2}e_1^2 - \frac{1}{2}(e_1 - \boldsymbol{c}^T\boldsymbol{\varepsilon})^2 - K_1v_1^2 - K_2v_2^2 \\ &+v_{3f}v_2 + (w_{3d} - \omega)v_2 + \sigma\tilde{\boldsymbol{\theta}}^T\hat{\boldsymbol{\theta}},\end{aligned} \quad (48)$$

and (39) as

$$\dot{v}_2 = -K_2v_2 - v_1 + \frac{1}{2}\boldsymbol{\alpha}^T\boldsymbol{R}^{-1}\boldsymbol{s_1} - \frac{1}{2}\boldsymbol{\alpha}^T\boldsymbol{R}^{-1}\boldsymbol{\alpha}v_2 + K_1\boldsymbol{\alpha}^T\left(\boldsymbol{\varepsilon} + \boldsymbol{P}^T\tilde{\boldsymbol{\theta}}\right) + v_{3f} + w_{3d} - \omega. \quad (49)$$

As $\dot{v}_{3f} = \dot{\omega} - \dot{w}_3$, Equation (46) and the last equation in (22) allow us to write down

$$\dot{v}_{3f} = \Omega(w_{3d} - \omega) - \boldsymbol{\Theta}^T\boldsymbol{H}(\boldsymbol{w}) - h(\boldsymbol{w}) - u \quad (50)$$

The control u is used to cancel inconvenient nonlinearities in (50), to stabilize the trajectory v_{3f}, and to original components, canceling inconvenient terms in the Lyapunov function derivative. Unknown slave system parameters $\boldsymbol{\Theta}$ are substituted by adaptive parameters $\widehat{\boldsymbol{\Theta}}$, and the adaptation error is defined as $\widetilde{\boldsymbol{\Theta}} = \boldsymbol{\Theta} - \widehat{\boldsymbol{\Theta}}$. All those reasons explain the following selection:

$$u = \Omega(w_{3d} - \omega) - \widehat{\boldsymbol{\Theta}}^T \boldsymbol{H}(\boldsymbol{w}) - h(\boldsymbol{w}) + K_3 v_{3f} + v_2. \tag{51}$$

Under control (51), Equation (50) is simplified as

$$\dot{v}_{3f} = -\widetilde{\boldsymbol{\Theta}}^T \boldsymbol{H}(\boldsymbol{w}) - K_3 v_{3f} - v_2. \tag{52}$$

The Lyapunov function for the whole system is chosen as

$$\begin{aligned} V_3 = V_2 + \frac{1}{2} v_{3f}^2 + \frac{\mathbf{1}}{\mathbf{2}} \widetilde{\boldsymbol{\Theta}}^T \boldsymbol{\Gamma}_{\mathbf{1}}^{-\mathbf{1}} \widetilde{\boldsymbol{\Theta}} \\ = \frac{1}{2} v_1^2 + \frac{1}{2} v_2^2 + \frac{1}{2} v_{3f}^2 + \frac{1}{2} \widetilde{\boldsymbol{\theta}}^T \boldsymbol{\Gamma}^{-\mathbf{1}} \widetilde{\boldsymbol{\theta}} + \boldsymbol{\varepsilon}^T \boldsymbol{R} \boldsymbol{\varepsilon} + \frac{1}{2} \widetilde{\boldsymbol{\Theta}}^T \boldsymbol{\Gamma}_1^{-1} \widetilde{\boldsymbol{\Theta}}. \end{aligned} \tag{53}$$

As $\dot{V}_3 = \dot{V}_2 + v_{3f} \dot{v}_{3f} - \widetilde{\boldsymbol{\Theta}}^T \boldsymbol{\Gamma}_1^{-\mathbf{1}} \dot{\widehat{\boldsymbol{\Theta}}}$, after plugging in (48) and (52), we obtain

$$\begin{aligned} \dot{V}_3 = -\boldsymbol{\varepsilon}^T \left(\boldsymbol{Q} - \frac{1}{2} \boldsymbol{c} \boldsymbol{c}^T \right) \boldsymbol{\varepsilon} - \frac{1}{2} e_1^2 - \frac{1}{2} (e_1 - \boldsymbol{c}^T \boldsymbol{\varepsilon})^2 - K_1 v_1^2 - K_2 v_2^2 + v_{3f} v_2 \\ + (w_{3d} - \omega) v_2 + \sigma \widetilde{\boldsymbol{\theta}}^T \widehat{\boldsymbol{\theta}} + v_{3f} \left(-\widetilde{\boldsymbol{\Theta}}^T \boldsymbol{H}(\boldsymbol{w}) - K_3 v_{3f} - v_2 \right) - \widetilde{\boldsymbol{\Theta}}^T \boldsymbol{\Gamma}_1^{-\mathbf{1}} \dot{\widehat{\boldsymbol{\Theta}}}. \end{aligned} \tag{54}$$

The robust adaptive law $\dot{\widehat{\boldsymbol{\Theta}}}$ is used to cancel the components containing $\widetilde{\boldsymbol{\Theta}}$; hence,

$$\dot{\widehat{\boldsymbol{\Theta}}} = \boldsymbol{\Gamma}_1 \left(-\boldsymbol{H}(\boldsymbol{w}) v_{3f} - \sigma_1 \widehat{\boldsymbol{\Theta}} \right) \tag{55}$$

and $\sigma_1 > 0$ is a small design parameter.

Substituting (50) and having in mind that $(w_{3d} - \omega) v_2 \le 0.5\rho + 0.5 v_2^2$ and $\widetilde{\boldsymbol{\theta}}^T \widehat{\boldsymbol{\theta}} = 0.5 \left(-\|\widetilde{\boldsymbol{\theta}}\|^2 + \|\boldsymbol{\theta}\|^2 - \|\widehat{\boldsymbol{\theta}}\|^2 \right)$, and that analogous equality holds for $\widetilde{\boldsymbol{\Theta}}^T \widehat{\boldsymbol{\Theta}}$, we obtain

$$\begin{aligned} \dot{V}_3 = -\boldsymbol{\varepsilon}^T \left(\boldsymbol{Q} - \frac{1}{2} \boldsymbol{c} \boldsymbol{c}^T \right) \boldsymbol{\varepsilon} - \frac{1}{2} e_1^2 - \frac{1}{2} (e_1 - \boldsymbol{c}^T \boldsymbol{\varepsilon})^2 - K_1 v_1^2 - K_2 v_2^2 + \sigma_1 \widetilde{\boldsymbol{\Theta}}^T \widehat{\boldsymbol{\Theta}} \\ \le -\boldsymbol{\varepsilon}^T \left(\boldsymbol{Q} - \frac{1}{2} \boldsymbol{c} \boldsymbol{c}^T \right) \boldsymbol{\varepsilon} - K_3 v_{3f}^2 + (w_{3d} - \omega) v_2 + \sigma \widetilde{\boldsymbol{\theta}}^{\boldsymbol{T}} \widehat{\boldsymbol{\theta}} - \frac{1}{2} e_1^2 - \frac{1}{2} (e_1 - \boldsymbol{c}^T \boldsymbol{\varepsilon})^2 \\ -K_1 v_1^2 - \left(K_2 - \frac{1}{2} \right) v_2^2 - K_3 v_{3f}^2 - \frac{\sigma}{2} \|\widetilde{\boldsymbol{\theta}}\|^2 - \frac{\sigma_1}{2} \|\widetilde{\boldsymbol{\Theta}}\|^2 + \frac{\rho}{2} + \frac{\sigma}{2} \|\boldsymbol{\theta}\|^2 + \frac{\sigma_1}{2} \|\boldsymbol{\Theta}\|^2. \end{aligned} \tag{56}$$

6. Closed-Loop System Stability

If the matrix $\boldsymbol{Q}$ is such that $\boldsymbol{Q} - 0.5 \boldsymbol{c} \boldsymbol{c}^T$ is positive definite and $K_2 > 0.5$, then according to (56), the Lyapunov function derivative becomes negative outside a certain compact set Δ in the state space of the aggregated state vector

$$\xi = \left[\boldsymbol{\varepsilon}, v_1, v_2, v_{3f}, \widetilde{\boldsymbol{\theta}}, \widetilde{\boldsymbol{\Theta}} \right]. \tag{57}$$

According to the well-known extension of the Lyapunov theorem [37], all signals in (57) are bounded and uniformly ultimately bounded to Δ. A designer is able to decrease the volume of Δ increasing the design parameters K_1, K_2, and K_3 and, therefore, to shape trajectories of v_1, v_2, and v_{3f}. Practical or numerical problems may be the only limit for the growth of K_1, K_2, and K_3. As the actual parameters $\boldsymbol{\theta}$ and $\boldsymbol{\Theta}$ are bounded, boundedness of adaptive parameters $\widehat{\boldsymbol{\theta}}, \widehat{\boldsymbol{\Theta}}$ follows from the boundedness of adaptation errors $\widetilde{\boldsymbol{\theta}}, \widetilde{\boldsymbol{\Theta}}$. The matrix $\boldsymbol{P}$ is generated as an output of a stable linear system (10), subject to the bounded excitation (as y is bounded); therefore, it is bounded itself. Hence, both $\widehat{\boldsymbol{\theta}}$ and $\dot{\widehat{\boldsymbol{\theta}}} = \boldsymbol{\Gamma} \boldsymbol{P} (\boldsymbol{c} e_1 + \boldsymbol{\alpha} v_1 + K_1 \boldsymbol{\alpha} v_2) - \sigma \boldsymbol{\Gamma} \widehat{\boldsymbol{\theta}}$ are bounded. Consequently, the observer (4) may be considered as the stable linear system ($\boldsymbol{A}_{\mathbf{0}}$ is stable) with the bonded input; hence, $\hat{\boldsymbol{z}}$ is bounded. Finally, both stabilizing functions w_{2d}, w_{3d} are bounded, and therefore, boundedness of w_1, w_2, and ω follows from the fact that v_1, v_2, and v_{3f} are bounded. Inspection of (51) assures that the control is also bounded as a sum of bounded components.

To summarize, the slave state variable w_1 follows the master output y, the tracking accuracy may be arbitrarily improved, and all signals in the closed-loop system remain bounded.

7. Example

We considered the Arneodo system (13) as the master system. With parameters $a = 7.5$, $b = 3.8$ it demonstrates chaotic motion. The evolution in chaotic regime is shown in Figure 2. At $t = 100$ [s], the input r changes from 0 to 4. Hence, the attractor moves along x_1 axis. For $t = 140$ [s], the value of parameter a changes from $a = 7.5$ to $a = 6.75$, transforming chaotic motion into a limit cycle (Figures 3–6). The transformation to the ONP form is defined by (16) and (19).

In the following, we present two numerical experiments, selected from many performed. In the first experiment, the properties of the designed adaptive observer were checked. The second experiment presents the results of the proposed synchronization algorithm of two different chaotic systems.

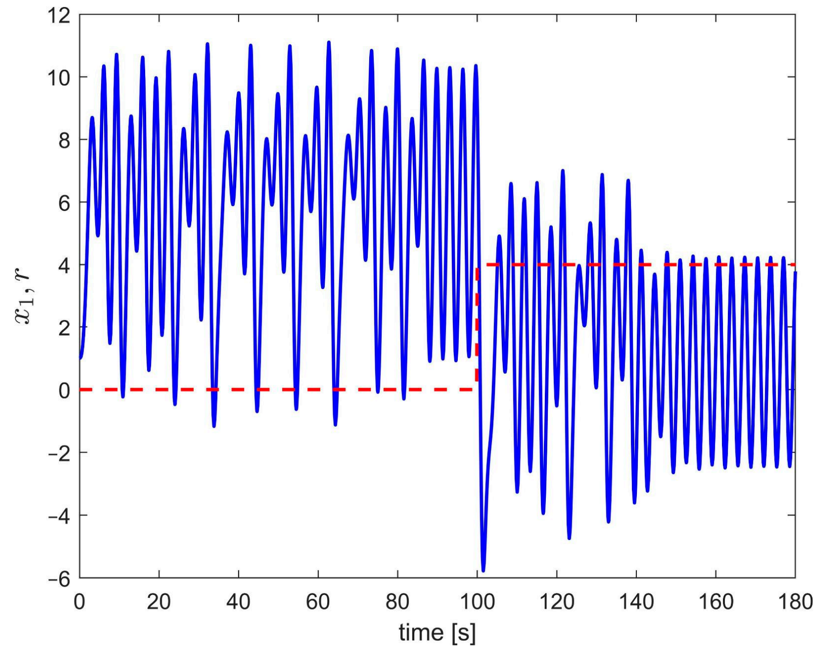

Figure 2. Evolution of signals $\boldsymbol{x_1}$ (solid line) and $\boldsymbol{r}$ (dashed line) for initial condition $\boldsymbol{x} = [\mathbf{1\ 0\ 0}]^{\boldsymbol{T}}$.

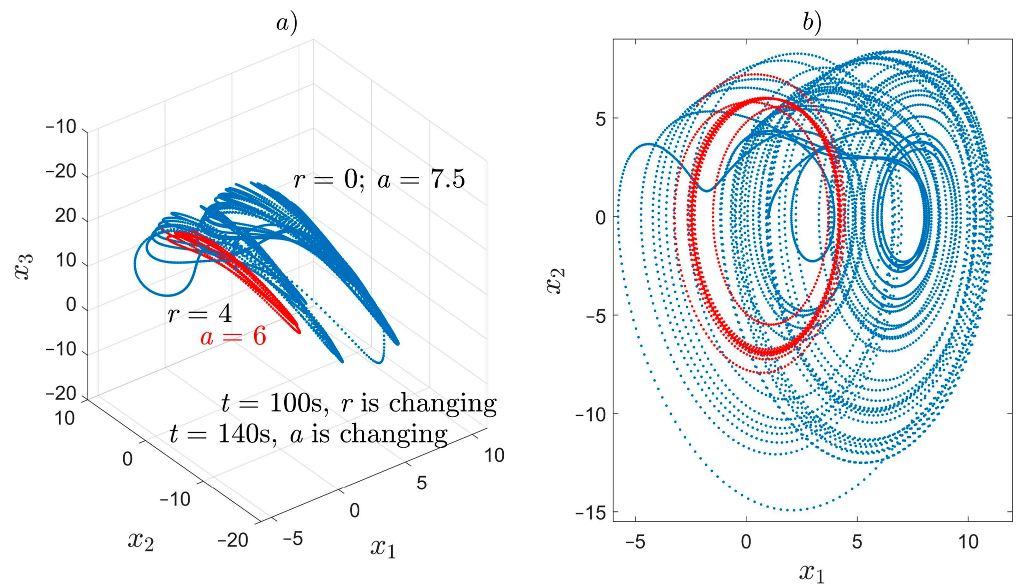

Figure 3. (**a**) State–space trajectories for initial condition $\boldsymbol{x} = [1\ 0\ 0]^T$; (**b**) a 2D projection of the state–space trajectories with Figure 3a on (x_1, x_2) plane.

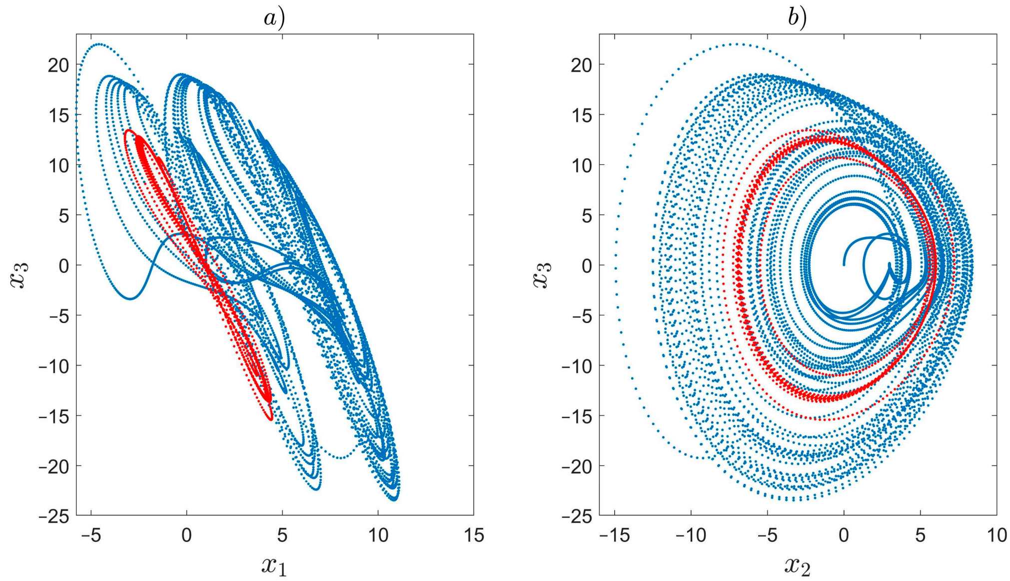

Figure 4. (**a**) A 2D projection of the state–space trajectories presented in Figure 3a on (x_1, x_3) plane; (**b**) a 2D projection of the state–space trajectories presented in Figure 3a on (x_2, x_3) plane.

7.1. Example 1—Observer Performance

First, we demonstrate features of the observer designed in Section 2. The tuning of the observer starts with placing the eigenvalues of $\boldsymbol{A_0}$ by an appropriate selection of gains $\boldsymbol{k}$. In this way, the dynamics of the linear part of the observer is decided. The speed of adaptation, which depends on $\boldsymbol{\Gamma}$, must correspond with the observer "time constant" defined by the maximal eigenvalue of $\boldsymbol{A_0}$—i.e., faster observer requires faster adaptation (higher $\boldsymbol{\Gamma}$). Matrices $\boldsymbol{Q}$ and $\boldsymbol{R}$, although used in the Lyapunov function (12) and its derivative (13), do not influence the observer directly.

The plots below are obtained for initial conditions of the Arneodo system $\boldsymbol{x}^T(0) = [1\ 0\ 0]$; hence, for the transformed system $\boldsymbol{z}(0) = \boldsymbol{\Phi x}(0) = [1\ 1\ 3.8]^T$, and initial conditions for the observer were selected as $\hat{\boldsymbol{z}}(0) = 0.8\boldsymbol{z}(0) = [0.8\ 0.8\ 3.04]^T$. The initial conditions for adaptive parameters were selected 20% lower than the real values.

Results of experiments shown in Figures 5 and 6 are typical for the obtained observer performance. All errors considered $(\boldsymbol{\varepsilon}, \boldsymbol{e}, \tilde{\boldsymbol{\theta}})$ converge to zero. By calculation of $\hat{\boldsymbol{x}} = \boldsymbol{\Phi}^{-1}(\hat{\boldsymbol{\theta}})\hat{\boldsymbol{z}}$, it is verified that $\boldsymbol{x} - \hat{\boldsymbol{x}} \to 0$, so the proposed observer provides estimates of original state variables $\boldsymbol{x}$ as well. This is demonstrated in Figure 5, in which the influence of design parameters is also illustrated. The highest estimation errors are observed just after the start of the system. Errors caused by shifting the attractor (change in r) are far smaller. A rapid change in the unknown parameter a, although it is not expected according to initial assumptions, is well tolerated. The observer recovers after such disturbance and returns to a perfect estimation of state variables.

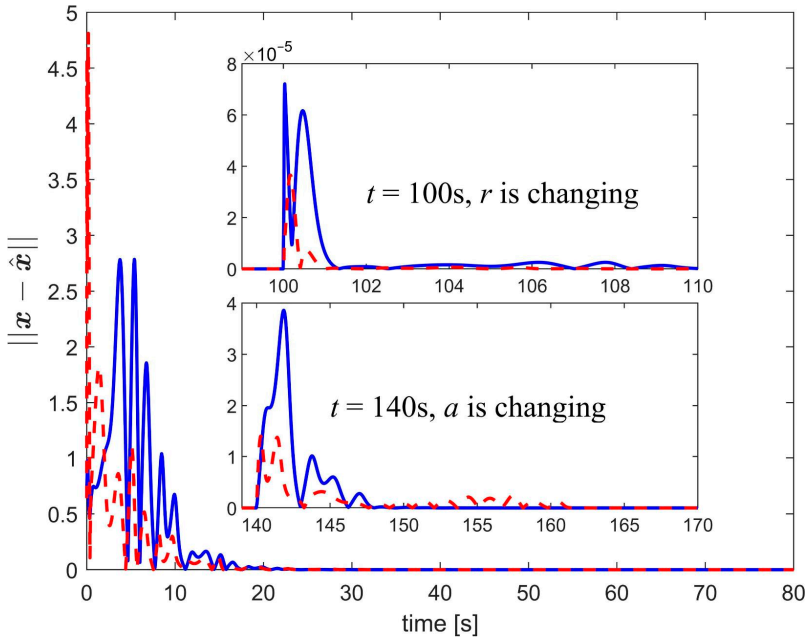

Figure 5. Norm of $||\boldsymbol{x} - \hat{\boldsymbol{x}}||$, design parameters: $\boldsymbol{k}^T$ = [15 75 125], providing triple eigenvalue of $\boldsymbol{A}_0$ at -5, $\boldsymbol{\Gamma} = diag(800; 1600)$, solid line; design parameters: $\boldsymbol{k}^T$ = [30 300 1000], providing triple eigenvalue of $\boldsymbol{A}_0$ at -10, $\boldsymbol{\Gamma} = diag(80\,000; 160\,000)$, dashed line.

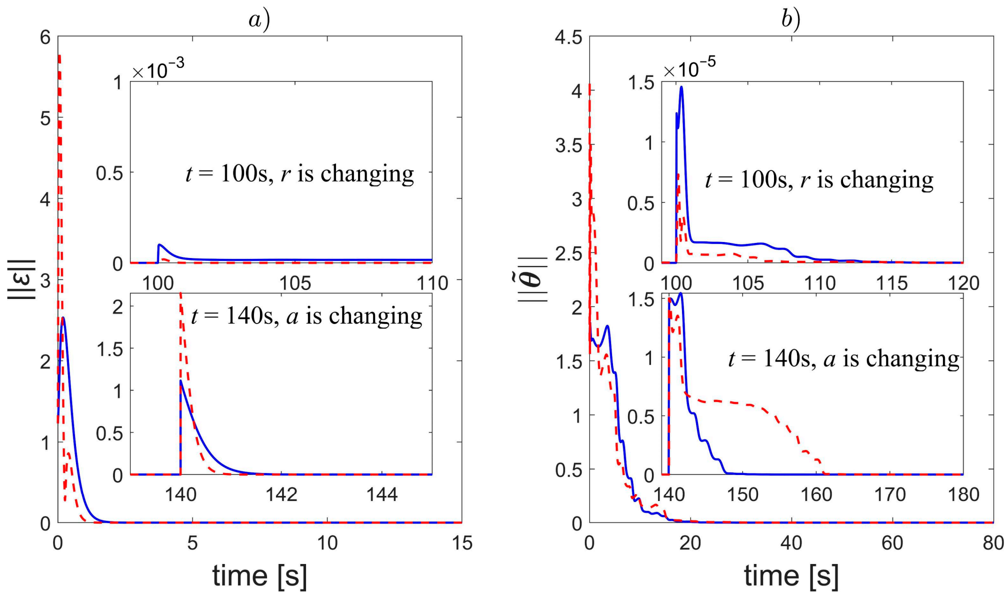

Figure 6. (**a**) Norm of the "composite" error $\boldsymbol{\varepsilon}$; (**b**) norm of parameter estimation errors; design parameters: $\boldsymbol{k}^T$ = [15 75 125], providing triple eigenvalue of $\boldsymbol{A}_0$ at -5, $\boldsymbol{\Gamma} = diag(800; 1600)$, solid line; design parameters: $\boldsymbol{k}^T$ = [30 300 1000], providing triple eigenvalue of $\boldsymbol{A}_0$ at -10, $\boldsymbol{\Gamma} = diag(80\,000; 160\,000)$, dashed line.

Figure 6a illustrates the nature of the "composite" error $\boldsymbol{\varepsilon}$. The chaotic motion is eliminated from this signal, and it converges exponentially according to Equation (11).

From 6b, we infer that the observer provides a good estimation of unknown parameters as well. After the initial transient, the estimates remain accurate and robust against the input signal changes.

Although the observer working alone behaves properly, the main aim is cooperation with the feedback controller, according to the structure presented in Figure 1.

7.2. Example 2—Synchronization

The slave system is the 3D jerk system described by Equations (22) and (23). With parameters $a = 3.6,\ b = 1.3,\ c = 0.1$, it demonstrates chaotic behavior. Evolution in chaotic regime is shown in Figure 7. Trajectories of the uncontrolled slave system are relatively far from those of the master system, even if started from the same initial conditions.

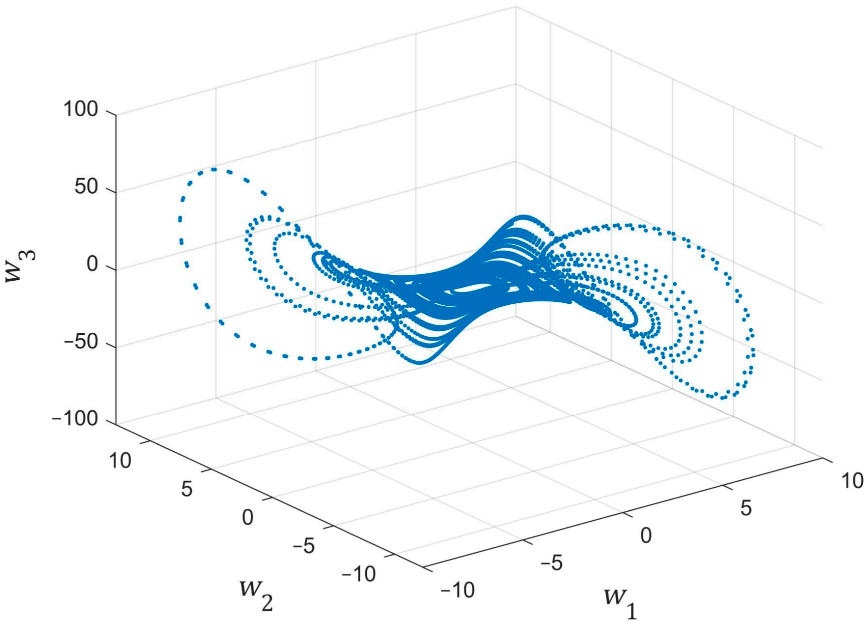

Figure 7. State–space trajectories of 3D Jerk system for initial condition $\boldsymbol{w} = [1\ 0\ 0]^T$.

Parameters of the observer were selected as $\boldsymbol{k}^T = [60\ 1200\ 8000]$ (providing a triple eigenvalue of $\boldsymbol{A_0}$ at -20), $\boldsymbol{\Gamma} = diag(8; 16),\ \sigma = 10^{-6}$. The observer's initial condition is $\hat{\boldsymbol{z}}(0) = [0.8\ 0.8\ 3.04]^T$. Parameters of the adaptive controller were chosen as $\boldsymbol{\Gamma_1} = diag(1; 2; 1)$ and $\sigma_1 = 0{,}0001$. Initial conditions of all adaptive parameters (in the observer and in the controller) were selected 20% lower than the real values. The filter parameter is $\Omega = 10^4$. Typical plots obtained from experiments are shown in Figures 8–10.

The proposed controller offers a fast response during the initial period of time and a small steady-state error. Increasing design parameters K_i results in reducing quasi-steady-state errors. The synchronization error $x_3 - w_3$ is larger than $x_2 - w_2$. It is caused by the application of the filter (46); $\Omega(w_{3d} - \omega)$ substitutes the accurate value of $\dot{w}_{3d}$ in (51).

The transient state of the synchronization process is even faster than state variables estimation by the observer alone. The feedback from the tracking errors improves the operation of the observer, and cooperation in the observer–controller loop results in high-quality synchronization.

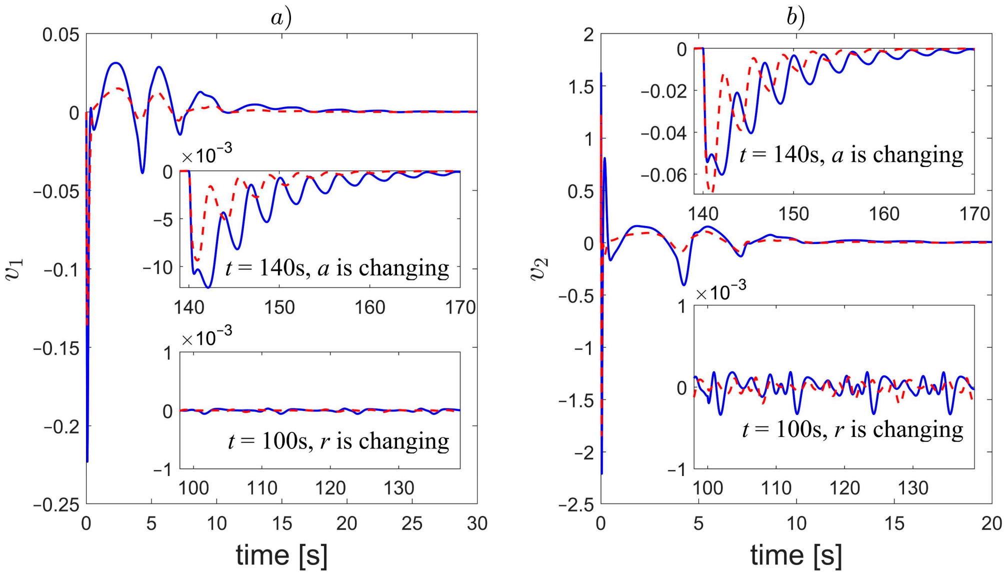

Figure 8. (**a**) Tracking/synchronization error $v_1 = x_1 - w_1$; (**b**) tracking error v_2; design parameters: $K_1 = K_2 = K_3 = 10$, solid line; design parameters: $K_1 = K_2 = K_3 = 15$, dashed line.

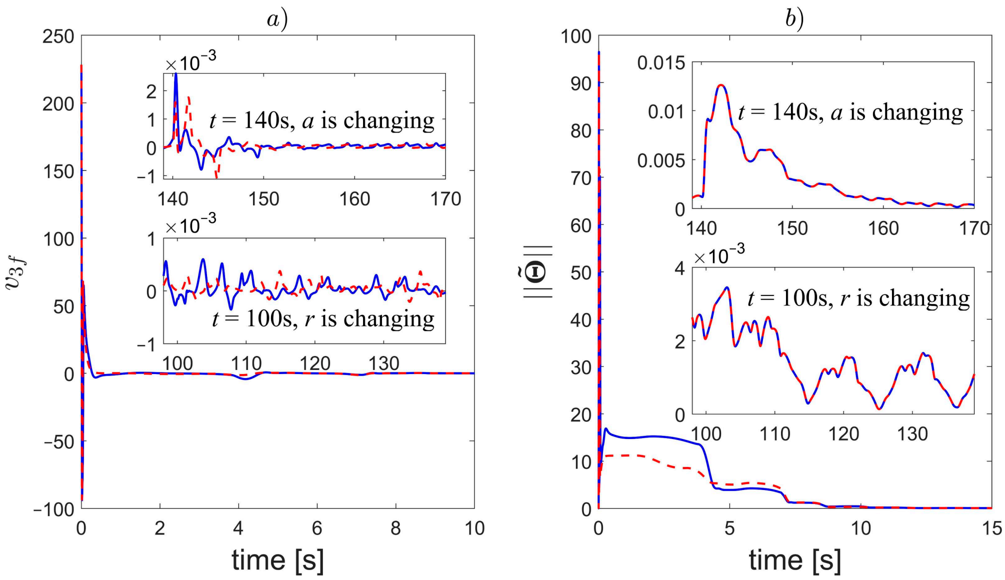

Figure 9. (**a**) Tracking error v_{3f}; (**b**) norm of parameter estimation errors $\|\tilde{\boldsymbol{\Theta}}\|$; design parameters: $K_1 = K_2 = K_3 = 10$, solid line; design parameters: $K_1 = K_2 = K_3 = 15$, dashed line.

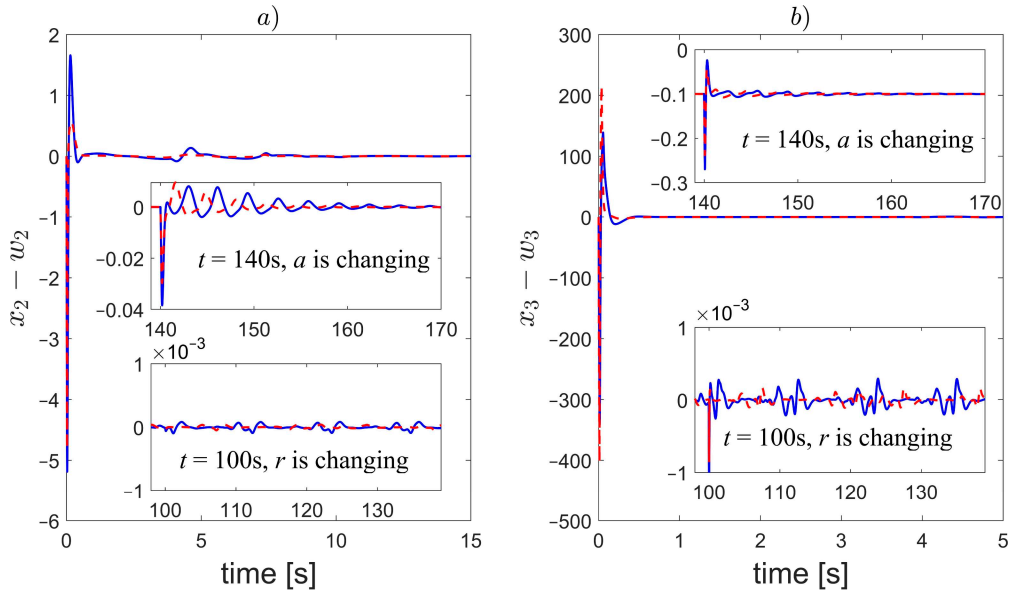

Figure 10. (**a**) Synchronization error $x_2 - w_2$; (**b**) synchronization error $x_3 - w_3$; design parameters: $K_1 = K_2 = K_3 = 10$, solid line; design parameters: $K_1 = K_2 = K_3 = 15$, dashed line.

8. Conclusions

The problem of the observer-based master–slave synchronization of completely different chaotic systems was solved under a novel set of assumptions. A modification of the K-filter-based observer was proposed, including feedback from the tracking adaptive controller. The master and the slave are connected by a single signal, which is a practical advantage in prospectus secure communication applications.

The main, new idea of the proposed approach is to enable cooperation between the adaptive observer and the adaptive tracking controller in a unified closed-loop system. Tracking errors fed back from the controller influence the observer (by a tuning function in adaptive law), improving the overall performance. Application of the tuning functions technique allows us to avoid overparameterization of the whole system—the number of adaptive parameters is the same as the number of unknown parameters. As a result of filter application, the "explosion of complexity" in the control law is prevented. The applied adaptive laws are robust; therefore, an uncontrolled increase in adaptive parameters is avoided.

The proposed controller can synchronize different chaotic systems with sufficient accuracy. Tuning of the design parameters is logical and clear. A designer can trade off the synchronization accuracy against the aggressiveness of the control strategy. The proposed solution was compared with adaptive tracking using all master–state–vector variables. The analyzed examples demonstrate that the obtained accuracy of tracking (synchronization) was similar, despite the smaller amount of information transferred from the master. Additionally, settling time, overshoot, and other control quality measures are comparable to those obtained in the case of full availability of the state vector. The same conclusions can be drawn from the comparison with the results presented in [11].

The selection of a particular type of nonlinear adaptive observer constrains the class of chaotic systems under consideration. In future research, we plan to explore other types of nonlinear adaptive observers in collaboration with a tracking controller. Although this paper concerns particular chaotic systems and the derivation concentrates on third-order systems, the proposed design technique may be easily adapted to different cases of nonlinear systems.

Author Contributions: Main idea, J.K. and P.M.; methodology, J.K. and P.M.; simulations, P.M.; validation, J.K. and P.M.; writing—original draft preparation, J.K. and P.M.; writing—review and editing, J.K.; visualization, P.M. All authors have read and agreed to the published version of the manuscript.

Funding: This research was funded by the Politechnika Łódzka (Lodz University of Technology) The APC was funded by Politechnika Łódzka.

Institutional Review Board Statement: Not applicable.

Informed Consent Statement: Not applicable.

Data Availability Statement: Not applicable.

Conflicts of Interest: The authors declare no conflicts of interest.

Appendix A

Let us consider a third-order system

$$\begin{gathered}\dot{x}_1 = x_2,\\ \dot{x}_2 = x_3,\\ \dot{x}_3 = f_0(x_1, \boldsymbol{r}) + \boldsymbol{\theta}^{\boldsymbol{T}}\boldsymbol{D}(\boldsymbol{x} + \boldsymbol{B}\boldsymbol{r}) + \boldsymbol{g}^{\boldsymbol{T}}\boldsymbol{x},\end{gathered} \tag{A1}$$

with the input $\boldsymbol{r}$, output $y = x_1$, state variables $\boldsymbol{x} = [x_1, x_2, x_3]^{\boldsymbol{T}}$, where $\boldsymbol{\theta}$ are unknown, constant parameters and $f_0(x, \boldsymbol{r}), \boldsymbol{D}, \boldsymbol{B}, \boldsymbol{g}^{\boldsymbol{T}}$ are known, and let us define state transformation

$$\boldsymbol{z} = \boldsymbol{T}\boldsymbol{x}, \qquad \boldsymbol{T} = \begin{bmatrix} 1 & 0 & 0 \\ \alpha & 1 & 0 \\ \beta & \gamma & 1 \end{bmatrix}. \tag{A2}$$

The inverse transformation is given by

$$\boldsymbol{x} = \boldsymbol{T}^{-\boldsymbol{1}}\boldsymbol{z}, \qquad \boldsymbol{T}^{-\boldsymbol{1}} = \begin{bmatrix} 1 & 0 & 0 \\ -\alpha & 1 & 0 \\ -\beta + \alpha\gamma & -\gamma & 1 \end{bmatrix}. \tag{A3}$$

Therefore, as

$$\boldsymbol{T}\begin{bmatrix} 0 \\ 0 \\ 1 \end{bmatrix} = \begin{bmatrix} 0 \\ 0 \\ 1 \end{bmatrix}, \tag{A4}$$

we have

$$\dot{\boldsymbol{z}} = \boldsymbol{T}\begin{bmatrix} [0 \quad 1 \quad 0] \\ [0 \quad 0 \quad 1] \\ \boldsymbol{\theta}^{\boldsymbol{T}}\boldsymbol{D} + \boldsymbol{g}^{\boldsymbol{T}} \end{bmatrix}\boldsymbol{T}^{-\boldsymbol{1}}\boldsymbol{z} + \begin{bmatrix} 0 \\ 0 \\ f_0(z_1, r) \end{bmatrix} + \begin{bmatrix} 0 \\ 0 \\ \boldsymbol{\theta}^{\boldsymbol{T}}\boldsymbol{D}\boldsymbol{B}\boldsymbol{r} \end{bmatrix}. \tag{A5}$$

Simple matrix manipulations provide that the last columns of the state matrix in (A5) are

$$\boldsymbol{T}\begin{bmatrix} [0 \quad 1 \quad 0] \\ [0 \quad 0 \quad 1] \\ \boldsymbol{\theta}^{\boldsymbol{T}}\boldsymbol{D} + \boldsymbol{g}^{\boldsymbol{T}} \end{bmatrix}\boldsymbol{T}^{-\boldsymbol{1}} = \begin{bmatrix} * & 1 & 0 \\ * & \alpha - \gamma & 1 \\ * & \beta - \gamma^2 + (\boldsymbol{\theta}^{\boldsymbol{T}}\boldsymbol{D} + \boldsymbol{g}^{\boldsymbol{T}})\begin{bmatrix} 0 \\ 1 \\ -\gamma \end{bmatrix} & \gamma + (\boldsymbol{\theta}^{\boldsymbol{T}}\boldsymbol{D} + \boldsymbol{g}^{\boldsymbol{T}})\begin{bmatrix} 0 \\ 0 \\ 1 \end{bmatrix} \end{bmatrix}, \tag{A6}$$

Therefore, the system (A1) is transformed into the ONP form if

$$\begin{gathered} q_1 = \alpha - \gamma, \\ q_2 = \beta - \gamma^2 + (\boldsymbol{\theta}^{\boldsymbol{T}}\boldsymbol{D} + \boldsymbol{g}^{\boldsymbol{T}})\begin{bmatrix} 0 \\ 1 \\ -\gamma \end{bmatrix}, \\ q_3 = \gamma + (\boldsymbol{\theta}^{\boldsymbol{T}}\boldsymbol{D} + \boldsymbol{g}^{\boldsymbol{T}})\begin{bmatrix} 0 \\ 0 \\ 1 \end{bmatrix} \end{gathered} \tag{A7}$$

do not depend on $\boldsymbol{\theta}$.

For Arneodo system (13)

$$\boldsymbol{\theta} = \begin{bmatrix} a \\ b \end{bmatrix}, \quad \boldsymbol{D} = \begin{bmatrix} 1 & 0 & 0 \\ 0 & -1 & 0 \end{bmatrix}, \quad \boldsymbol{B} = \begin{bmatrix} 1 \\ 0 \\ 0 \end{bmatrix}, \quad \boldsymbol{g}^{\boldsymbol{T}} = [0 \quad 0 \quad -1]. \tag{A8}$$

Therefore,

$$\boldsymbol{\theta}^{\boldsymbol{T}}\boldsymbol{D} + \boldsymbol{g}^{\boldsymbol{T}} = [a \quad -b \quad -1]. \tag{A9}$$

As $q_2 = \beta - \gamma^2 - b + \gamma$, selecting $\beta = b$ and any α, γ that do not depend on unknown parameters constitutes a family of transformations into the ONP form. One of them is $\alpha = 1, \beta = b, \gamma = 1$, applied in (14).

Therefore, the Arneodo system is linearly transformable into the ONP form. Additionally, several other popular chaotic systems such as Arneodo–Coullet [38], Genesio–Tesi [39], and Lur'e [35] belong to this class.

References

1. Pecora, L.M.; Carroll, T.L. Synchronization in Chaotic Systems. *Phys. Rev. Lett.* **1990**, *64*, 821–824. https://doi.org/10.1103/PhysRevLett.64.821.
2. Kun, G. A Synchronization Controller for the Unified Chaotic System and Its Application in Secure Communication. In Proceedings of the 2011 International Conference on Consumer Electronics, Communications and Networks (CECNet), Xianning, China, 11–13 March, 2011; pp.4700-4703.
3. Lin, X.; Zhou, S.; Zou, Z.; Li, Y. Chaos and Its Communication Application of Fractional-Order Neutral Differential System. In Proceedings of the 2010 International Workshop on Chaos-Fractal Theories and Applications, Kunming, China, 29-31 October 2010; pp.174-178
4. Yang, L.; Zhang, J. A New Multistage Chaos Synchronized System for Secure Communications and Noise Perturbation. In Proceedings of the 2009 International Workshop on Chaos-Fractals Theories and Applications; Shenyang, China, 6-8 November 2009; pp. 35–39.
5. Koltsova, E.M.; Cherenkov, M.V.; Korchagin, E.Y. Nonlinear Processes and Control of Chaos in Chemical Technology. In Proceedings of the 2003 IEEE International Workshop on Workload Characterization, Austin, TX, USA, 27 October 2003; Volume 2, pp. 484–490.
6. Frisman, E.Y.; Sycheva, E.V. Oscillations and Chaos in Population Dynamics Caused by Hunting. In Proceedings of the 2000 2nd International Conference. Control of Oscillations and Chaos, Saint Petersburg, Russia,5-7 July 2000; Volume 3, pp. 576–578.
7. Ji, W. Chaos and Control of Nonlinear Dynamic Model in the Ecological System. In Proceedings of the 2010 International Workshop on Chaos-Fractal Theories and Applications; Kunming, China, 29-31 October 2010; pp. 326–330.
8. Gómez-Pavón, L.C.; Muñoz-Pacheco, J.M.; Luis-Ramos, A. Synchronous Chaos Generation in an Er^{3+}-Doped Fiber Laser System. *IEEE Photonics J.* **2015**, *7*, 1–6. https://doi.org/10.1109/JPHOT.2015.2419073.
9. Roy, R. Coherence and Chaos in Solid State Laser Systems. In Proceedings of the LEOS '95. IEEE Lasers and Electro-Optics Society 1995 Annual Meeting. 8th Annual Meeting, San Francisco, CA, USA, 30-31 October 1995; Volume 1, pp. 155–156.
10. Zhang, H.; Huang, W.; Wang, Z.; Chai, T. Adaptive Synchronization between Two Different Chaotic Systems with Unknown Parameters. *Phys. Lett. A* **2006**, *350*, 363–366. https://doi.org/10.1016/j.physleta.2005.10.033.
11. Kabziński, J. Synchronization of an Uncertain Duffing Oscillator with Higher Order Chaotic Systems. *Int. J. Appl. Math. Comput. Sci.* **2018**, *28*, 625–634. https://doi.org/10.2478/amcs-2018-0048.
12. Guo, J.; Zhao, Z.; Shi, F.; Wang, R.; Li, S. Observer-Based Synchronization Control for Coronary Artery Time-Delay Chaotic System. *IEEE Access* **2019**, *7*, 51222–51235. https://doi.org/10.1109/ACCESS.2019.2909749.
13. Cui, D.; Xu, J. Synchronization of Chaotic Systems Having Triangular Structure via Observer. In Proceedings of the 2018 37th Chinese Control Conference (CCC); Wuhan, China, 25-27 July 2018; pp. 769–773.
14. Kocamaz, U.E.; Uyaroğlu, Y.; Kizmaz, H. Control of Rabinovich Chaotic System Using Sliding Mode Control. *Int. J. Adapt. Control Signal Processing* **2014**, *28*, 1413–1421. https://doi.org/10.1002/acs.2450.
15. Vaidyanathan, S.; Rasappan, S. Global Chaos Synchronization of N-Scroll Chua Circuit and Lur'e System Using Backstepping Control Design with Recursive Feedback. *Arab. J. Sci. Eng.* **2014**, *39*, 3351–3364. https://doi.org/10.1007/s13369-013-0929-y.
16. Singh, S.; Handa, H. Synchronization of MLS Chaotic System Using Adaptive Backstepping Control. In Proceedings of the 2020 7th International Conference on Signal Processing and Integrated Networks (SPIN), 27-28 February 2020; pp. 1084–1088.
17. Shukla, M.; Bansal, A.; Sharma, B.B. Synchronization of a Class of Non-Identical Chaotic Systems via DSC Approach. In Proceedings of the 2013 IEEE International Conference on Signal Processing, Computing and Control (ISPCC); Waknaghat, India, 26-28 September 2013; pp. 1–6.
18. Li, D.-J. Adaptive Output Feedback Control of Uncertain Nonlinear Chaotic Systems Based on Dynamic Surface Control Technique. *Nonlinear Dyn.* **2012**, *68*, 235–243. https://doi.org/10.1007/s11071-011-0222-0.

19. Zhang, J.; Cui, Q.; Zhao, Z.; Huo, S. Synchronization Control Design Based On Observers For Time-Delay Lur'e Systems. *IEEE Access* **2020**, *8*, 1–1. https://doi.org/10.1109/ACCESS.2020.2995082.
20. Cui, D.; Zhu, H.; Liu, H. Adaptive Fuzzy Control for a Class of Uncertain Chaotic Systems Based on Proportional-Integral Sliding Mode Control Approach. In Proceedings of the 2018 Chinese Control And Decision Conference (CCDC), Shenyang, China, 9-11 June 2018; pp. 589–593.
21. N'Doye, I.; Darouach, M.; Voos, H. Observer-Based Approach for Fractional-Order Chaotic Synchronization and Communication. In Proceedings of the 2013 European Control Conference (ECC), Zurich, Switzerland, 17-19 July 2013; pp. 4281–4286.
22. Borri, A.; Cacace, F.; Gaetano, A. de Germani, A.; Manes, C.; Palumbo, P.; Panunzi, S.; Pepe, P. Luenberger-Like Observers for Nonlinear Time-Delay Systems with Application to the Artificial Pancreas: The Attainment of Good Performance. *IEEE Control Syst.* **2017**, *37*, 33–49. https://doi.org/10.1109/MCS.2017.2696759.
23. Guay, M. Adaptive Gain Nonlinear Observer Design Techniques. In Proceedings of the 2017 6th International Symposium on Advanced Control of Industrial Processes (AdCONIP), Taipei, Taiwan, 28-31 May 2017; pp. 143–148.
24. Kazantzis, N.; Kravaris, C. A Nonlinear Luenberger-Type Observer with Application to Catalyst Activity Estimation. In Proceedings of the Proceedings of 1995 American Control Conference - ACC'95; American Autom Control Council, Seattle, WA, 21-23 June 1995; Volume 3, pp. 1756–1761.
25. Chernikova, O.S. An Adaptive Unscented Kalman Filter Approach for State Estimation of Nonlinear Continuous-Discrete System. In Proceedings of the 2018 XIV International Scientific-Technical Conference on Actual Problems of Electronics Instrument Engineering (APEIE), Novosibirsk, Russia, 2-6 October 2018; pp. 37–40.
26. Fei, J.; Hua, M. A Novel Design of Adaptive Sliding Mode Observer. In Proceedings of the 2010 8th World Congress on Intelligent Control and Automation, Jinan, China, 6-9 July 2010; pp. 843–848.
27. Vo, A.T.; Kang, H.-J.; Nguyen, V.-C. An Output Feedback Tracking Control Based on Neural Sliding Mode and High Order Sliding Mode Observer. In Proceedings of the 2017 10th International Conference on Human System Interactions (HSI), Ulsan, Korea, 17-19 July 2017; pp. 161–165.
28. Saad, M.; Liaquat, M. Output Regulation of Feedback Linearizable System (Single Link Robot Manipulator): A Cascaded High Gain Observer Approach. In Proceedings of the 2017 7th IEEE International Conference on Control System, Computing and Engineering (ICCSCE), Penang, Malaysia, 24-26 November 2017; pp. 226–229.
29. Khalil, H.K. Cascade High-Gain Observer for High-Dimensional Systems. In Proceedings of the 2016 IEEE 55th Conference on Decision and Control (CDC), Las Vegas, NV, 12-14 December 2016; pp. 7141–7146.
30. Wang, H.; Dong, Y.; Qin, W. Adaptive Observer Design for a Class of Lipschitz Nonlinear Systems. In Proceedings of the Proceedings of the 30th Chinese Control Conference, Yantai, China, 22-24 July 2011; pp. 665–669.
31. Hu, G.-D. Observers for One-Sided Lipschitz Non-Linear Systems. *IMA J. Math. Control Inf.* **2006**, *23*, 395–401. https://doi.org/10.1093/imamci/dni068.
32. Zhao, Y.; Zhang, W.; Su, H.; Yang, J. Observer-Based Synchronization of Chaotic Systems Satisfying Incremental Quadratic Constraints and Its Application in Secure Communication. *IEEE Trans. Syst. Man Cybern. Syst.* **2020**, *50*, 5221–5232. https://doi.org/10.1109/TSMC.2018.2868482.
33. Krstic, M.; Ioannis, K.; Kokotovic, P.V. *Nonlinear and Adaptive Control Design*; Wiley, New York, USA, 1995; ISBN 978-0-471-12732-1.
34. Kreisselmeier, G. Adaptive Observers with Exponential Rate of Convergence. *IEEE Trans. Autom. Control* **1977**, *22*, 2–8. https://doi.org/10.1109/TAC.1977.1101401.
35. Zhu, F.; Xu, J.; Chen, M. The Combination of High-Gain Sliding Mode Observers Used as Receivers in Secure Communication. *IEEE Trans. Circuits Syst. I: Regul. Pap.* **2012**, *59*, 2702–2712. https://doi.org/10.1109/TCSI.2012.2190570.
36. Gao, Y.-F.; Sun, X.-M.; Wen, C.; Wang, W. Observer-Based Adaptive NN Control for a Class of Uncertain Nonlinear Systems With Nonsymmetric Input Saturation. *IEEE Trans. Neural Netw. Learn. Syst.* **2017**, *28*, 1520–1530. https://doi.org/10.1109/TNNLS.2016.2529843.
37. Kabziński, J.; Mosiołek, P. *Projektowanie Nieliniowych Układów Sterowania (Nonlinear Control Design)*; I.; PWN SA: Warszawa, Poland, 2018; ISBN 978-83-01-19697-4.
38. Vaidyanathan, S. *Output Regulation of Arneodo-Coullet Chaotic System*. In Proceedings of the Advanced Computing; Meghanathan Natarajan and Kaushik, B.K. and N.D., Ed.; Springer Berlin Heidelberg: Berlin, Heidelberg, 2011; pp. 98–107.
39. Park, J.H. Synchronization of Genesio Chaotic System via Backstepping Approach. *Chaos Solitons Fractals* **2006**, *27*, 1369–1375. https://doi.org/10.1016/j.chaos.2005.05.001.
40. Mazenc, F.; Praly, L.; Dayawansa, W.P. Global Stabilization by Output Feedback: Examples and Counterexamples. *Syst. Control Lett.* **1994**, *23*, 119–125. https://doi.org/10.1016/0167-6911(94)90041-8.
41. Ioannou, P.; Sun, J. *Robust Adaptive Control*; DOVER PUBN INC, New York, USA, 2012; ISBN 978-0-486-49817-1.
42. Sastry, S.; Bodson, M. *Adaptive Control: Stability, Convergence, and Robustness*; Prentice Hall: Englewood Cliffs, N.J., USA, 1989; ISBN 0130043265.
43. Marino, R. Adaptive Observers for Single Output Nonlinear Systems. *IEEE Trans. Autom. Control* **1990**, *35*, 1054–1058. https://doi.org/10.1109/9.58536.
44. Vaidyanathan, S. A New 3-D Jerk Chaotic System with Two Cubic Nonlinearities and Its Adaptive Backstepping Control. *Arch. Control Sci.* **2017**, *27*, 409–439. https://doi.org/10.1515/acsc-2017-0026.